Reprinted from SPIE Vol. 902—Three-Dimensional Imaging and Remote Sensing Imaging

3-D Display of Magnetic Resonance Imaging of the Spine

Alan C. Nelson, Yongmin Kim*, Robert M. Haralick*, Paul A. Anderson**
Roger H. Johnson and Larry A. DeSoto*

University of Washington • Center for Bioengineering
and Departments of Electrical Engineering* and Orthopædics**
Seattle, WA 98195

ABSTRACT

The original data is produced through standard magnetic resonance imaging (MRI) procedures with a surface coil applied to the lower back of a normal human subject. The 3-D spine image data consists of twenty-six contiguous slices with 256 × 256 pixels per slice. Two methods for visualization of the 3-D spine are explored. One method utilizes a verifocal mirror system which creates a true 3-D virtual picture of the object. Another method uses a standard high resolution monitor to simultaneously show the three orthogonal sections which intersect at any user-selected point within the object volume. We discuss the application of these systems in assessment of low back pain.

1. Introduction

The potential for MRI to have a significant impact in health care associated with low back pain has been demonstrated[1], but physicians have agreed that improved methods for 3-D visualization of the spine with increased resolution and graphical manipulation are essential. Accordingly, we report on work which addresses the image processing and workstation requirements which would promote the specific application of MRI to the analysis of spinal malady particularly associated with low back pain.

Low back pain afflicts over 80% of all people during their lifetime. Usually the problem is self-limiting and recovery occurs within two months; however, a significant fraction of the work force is disabled with chronic low back pain. This medical problem accounts for 25% of all insurance claims and 40% of dollars paid out[2]. Current estimates suggest that approximately 15 billion dollars per year are lost due to reduced work productivity resulting from low back pain. The economic impact of spinal impairment is overwhelming, yet physicians generally are unable to perform accurate diagnosis to facilitate timely and effective treatment. Orthopaedic surgeons have realized that higher-resolution non-invasive 3–D imaging techniques will be essential in aiding diagnosis and that methods enabling soft tissue analysis in 3–D will contribute substantially to improved health care for afflicted individuals.

While various radiological imaging procedures result in a 3–D volume of data (e.g., CT, ultrasound, MRI), physicians typically view only one 2-D slice at a time. Methods for 3–D visualization are not well established, and consequently, 3–D data volumes are seldom visualized as such. In the context of MRI of the human spine, two workstation technologies are implemented to provide further insight into the problems of 3–D visualization: One technology uses the verifocal mirror to create a true 3–D virtual image, the other technology displays three 2-D orthogonal views whose intersection coincides with the location of a user-manipulable cursor which may be placed anywhere in the 3–D object volume. Advantages and limitations of these two systems are discussed.

2. Object Data

The original object data consists of 26 contiguous axial slices, each slice having a pixel resolution of 256 × 256. This translates to a spatial resolution of about 1.5mm in the plane of each slice whose thickness is about 1.5mm. The greyscale resolution is 12 bits. Our particular region of interest comprises the lower lumbar units of the spine. The data is generated using a single surface coil and the FLASH pulse sequence in MRI.

3. Image Processing

MRI images generated with a single surface coil will exhibit a strongly non-uniform greyscale distribution

across the image becoming brightest near the surface coil. It is possible to normalize the background greyscale by subtracting from the original data a model of the background contribution due to the surface coil. This model of the background can be obtained using sequential applications of morphological closings and openings on the original image data. Figure 1a shows an original data slice with the bright area adjacent to the surface coil placed on the patient's back. Figures 1b-d show the steps leading to the background image that is subtracted from the original image (Figure 1a) to produce the normalized image (Figure 1e) which has a flat background. The normalized slices can now be further processed to extract structural information relating to boundaries between tissue units (Figure 2). The image structural information is assembled in a file to facilitate 3–D display on the verifocal mirror system[3] (Figures 3a and 3b).

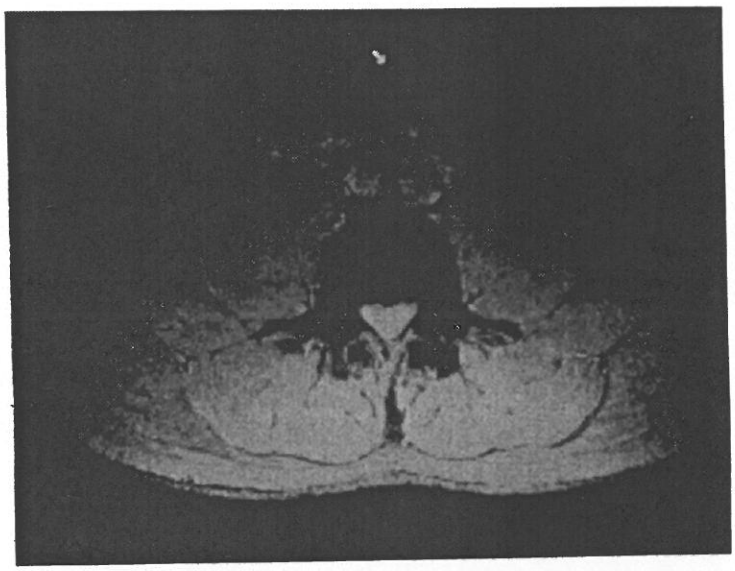

Figure 1a *shows original data. The bright area is adjacent to surface coil location placed on patient's back.*

Figure 1b *shows the result of performing a morphological closing using a relatively small square structuring element.*

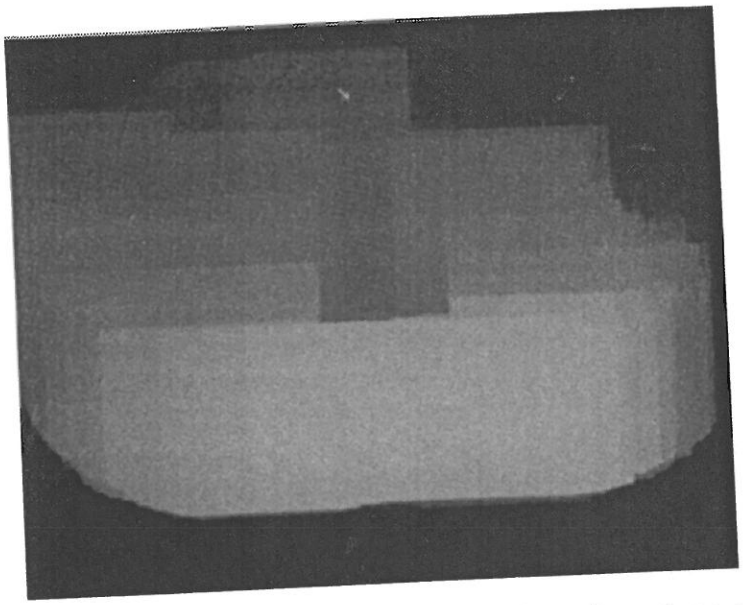

Figure 1c *illustrates the image of Figure 1b after a morphological opening using a relatively large square structuring element.*

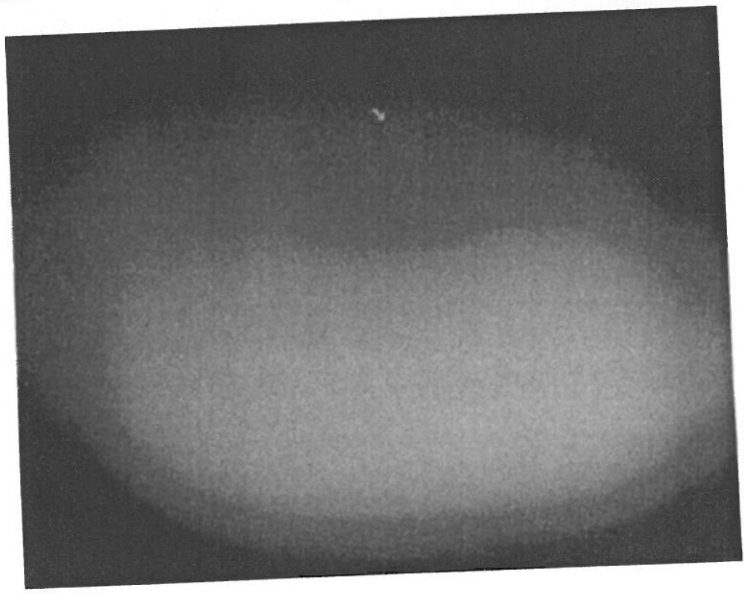

Figure 1d *shows the opened image after box filtering (averaging) with a structuring element comparable in size to that used for opening. This approximates the background.*

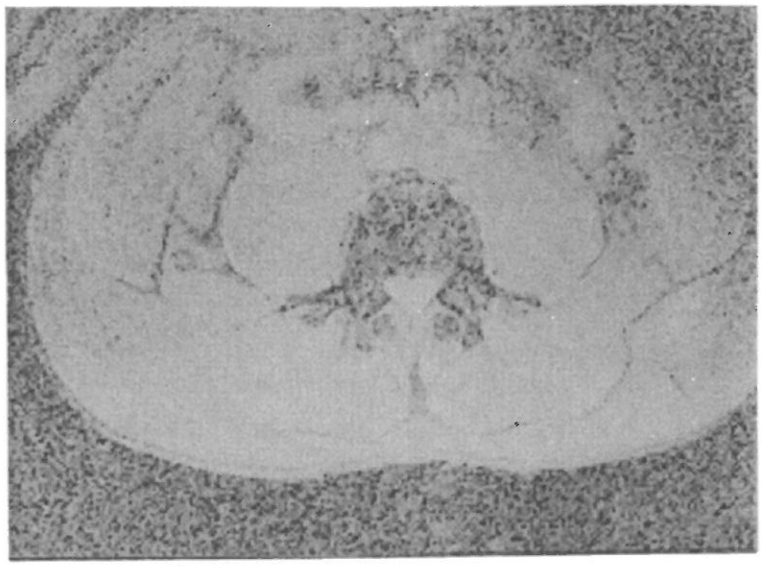

Figure 1e *illustrates the result of subtracting the background from the original.*

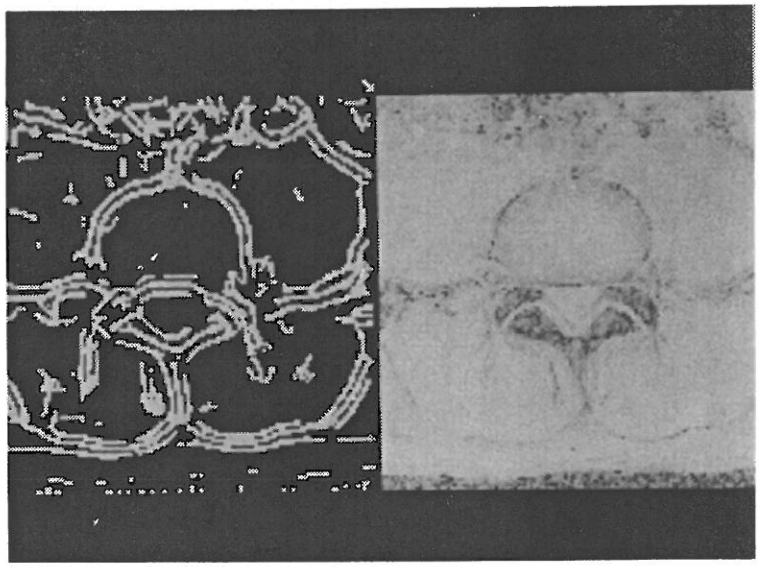

Figure 2 *shows the binary edges–plus–valleys image along with the processed image from which it is obtained.*

3.1 Background normalization

The normalization of the MR image background is accomplished using the tools of mathematical morphology, namely dilation and erosion, opening and closing[4]. The elementary operations of morphology are dilation and erosion, denoted $\oplus$ and $\ominus$, respectively. The binary dilation of a set A with a structuring element K is defined by

$$A \oplus K = \{x | \text{ for some } a \in A \text{ and } b \in K, x = a + b\}$$

The binary erosion of a set A with a structuring element is defined by

$$A \ominus K = \{x | \text{ for every } a \in A, x + a \in K\}$$

The greyscale dilation of a function $f : F \rightarrow (-\infty, \infty)$ with a structuring element $k : K \rightarrow (-\infty, \infty)$ is defined by

$$(f \oplus k)(x) = \max_{\substack{z \in K \\ x - z \in F}} [f(x - z) + k(z)]$$

for $x \in F \oplus K$.

The greyscale erosion of f by k is defined by

$$(f \ominus k)(x) = \min_{z \in K} [f(x + z) - k(z)]$$

for $x \in F \ominus K$

Dilation and erosion are duals in the sense that $(A \oplus K)^C = A^C \ominus \check{K}$ and $-(f \oplus k) = (-\check{f}) \ominus k$ where $\check{K} = \{z | -z \in K\}$ and $\check{h}(x) = \check{h}(-x)$.

The morphological operations are important because they have a natural relationship to shape. This becomes apparent when one considers the meaning of the composite morphological and dual operations of opening and closing. The opening of a set A by a structuring element K is defined by

$$A \circ K = (A \ominus K) \oplus K.$$

The closing of a set A by a structuring element K is defined by

$$A \bullet K = (A \oplus K) \ominus K$$

Likewise, the opening of a function f by a structuring element k is defined by

$$f \circ k = (f \ominus k) \oplus k$$

and the closing of a function f by a structuring element k is defined by

$$f \bullet k = (f \oplus k) \ominus k.$$

Opening and closing are both idempotent, that is, $(A \circ K) \circ K = A \circ K, (A \bullet K) \bullet K = A \bullet K, (f \circ k) \circ k = f \circ k$, and $(f \bullet k) \bullet k = f \bullet k$. They stand to morphology as the orthogonal projection operator stands to linear algebra. In linear algegbra, the orthogonal projection of x onto a subspace S is that part of x which lies in S. In morphology, $A \circ K$ is that subset of A which "matches" K. This notion of matching is precisely expressed in the morphological characterization theorem for opening:

$$A \circ K = \{x \in A | \text{ for some translation } t, x \in K_t \subseteq A\}$$

where

$$K_t = \{z | \text{ for some } y \in K, z = y + t\}.$$

The opening of A by K is precisely those points of A which can be covered by some translation of the structuring element K which itself is entirely contained in A. And this is what the primitive morphological

matching means. By duality $(A \circ K)^C = (A^C \bullet \check{K})$ so what opening with K does to the forground closing with $\check{K}$ does to the background.

Opening and closing with functions has a similar geometric meaning. The opening of a function f by a structuring element k can be visualized by sliding the structuring element k under f. The opening is given by the locus of the highest points reached by some part of k on the slide. By duality $-(f \circ k) = -f \bullet \check{k}$ so what opening with k does to f, closing with $\check{k}$ does to $-f$.

This characterization of opening and closing make them the ideal operations with which to perform background normalization to correct for shading variations in images. Let k designate the structuring element used for correcting the shading. If the domain of k is larger than any of the objects of interest or the image, then $f \circ k$ represents a lower envelope containing only those variations whose extent is larger than the domain of k. Since background normalization should be relatively smooth, we blur the opening by convolving it with a box filter b before subtracting it from f to eliminate the shading effect. Since an image may contain noise whose negative peaks would tend to push the lower envelope lower than where it would ideally be, or may contain small dark objects, we first close the image with a structuring element m just large enough to create an upper envelope which preserves all variations larger than the smallest dark object of interest. Then we determine the lower envelope of the upper envelope. Thus, the basic normalization is given by $g = f - [(f \bullet m) \circ k] * b$. For the MR images of the lower spine, m is the zero height constant function defined on a 16 × 16 neighborhood , k is the zero height constant function defined on a 50 × 50 neighborhood, and b is the constant function having height $\frac{1}{3600}$ over a 60 × 60 neighborhood.

3.2 Edge and line detection

The background-normalized images, one of which is shown in Figure 1e, are further processed to obtain structure delineation in each image slice. To detect edges and dark lines, we use the facet edge operator and ridge and valley operator[5,6]. The facet model principle of processing the image is that the digital image must be considered to be a noisy sampling of an underlying continuous greytone intensity surface. Features such as edges or lines are detected by first estimating each local underlying greytone intensity surface and then marking those points which satisfy the definition of edge or line with respect to the underlying greytone intensity surface. The facet model edge is defined to be any point having a negatively sloped zero crossing of the second directional derivative taken in the direction of the gradient. The facet model ridge or valley (light or dark lines) is defined to be any point having a zero crossing of the first directional derivative taken in the direction extremizing the second directional derivative.

The edge and valley image was prepared by first smoothing the image. A Gaussian filter with $\sigma = .61$ was followed by a 3 × 3 iterated box filter seven times. A bivariate cubic least squares facet fit was then done for every 5 × 5 neighborhood in the image. Pixels having a negatively sloped zero crossing of the second directional derivative taken in the direction of the gradient within a distance of .7 to the center of the pixel and having a contrast of at least 40 were marked as edges. Pixels having a zero crossing of the first directional derivative taken in a direction extremizing a positive second directional derivative within a distance of .85 to the center of the pixel were marked as valleys.

3.3 Extraction of structural information for 3–D display

Image processing with edge and valley detectors produces a binary image slice which can be stacked with all other registered binary slices to create an appropriate volume of data for display on the true 3–D verifocal mirror system (Spacegraph, Bolt Beranek and Newman, Inc., Cambridge, MA). An example of edge and valley extraction is shown in Figure 2 where a window 128 × 128 around the spine has been locally processed. When the binary files of image slices are appropriately stacked and displayed on the verifocal mirror system, a true 3–D virtual image emerges. Figures 3a and 3b are a left and right stereo pair which illustrate the 3–D effect when viewed in a stereoscope. Potentially important greyscale information is lost during this process.

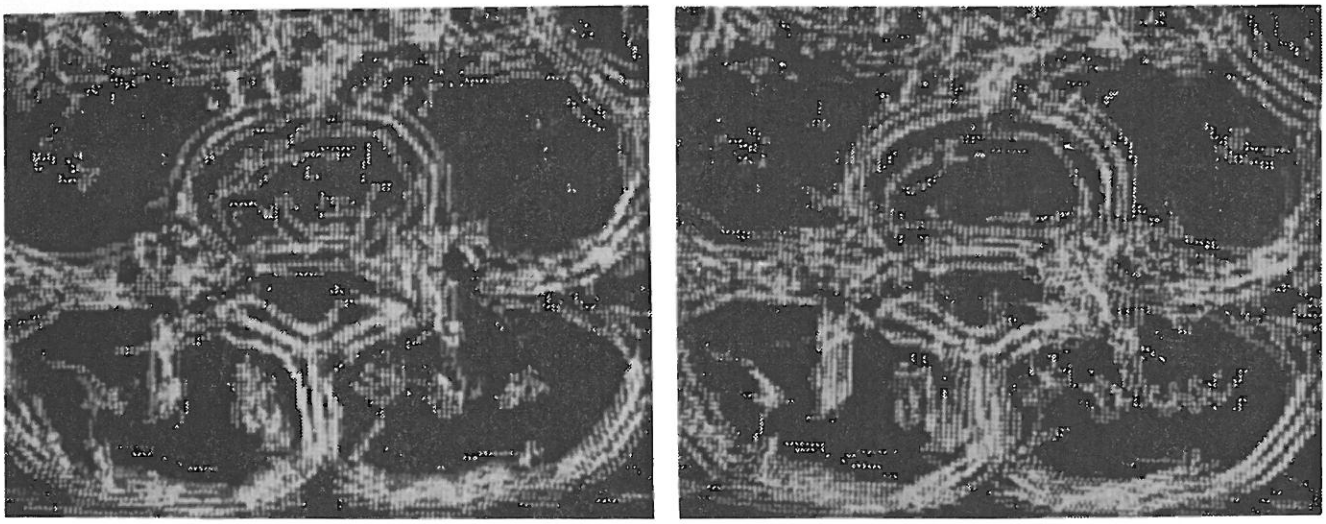

Figure 3a and 3b

Left and right stereo pair of four binary slices displayed simultaneously on the Spacegraph.

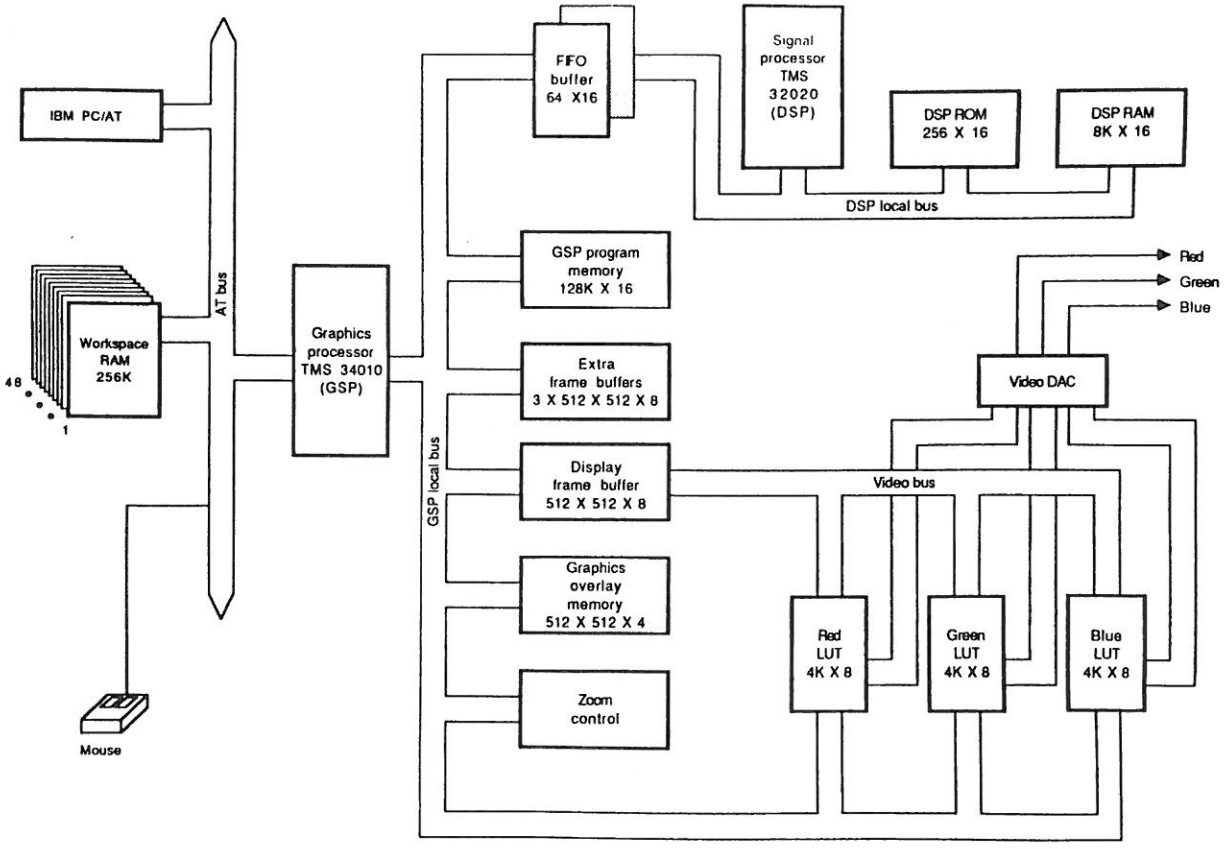

Figure 4 *illustrates a block diagram of the UWGSP system.*

4. Display of Three Orthogonal Views

In order to preserve greyscale image information and provide viewing of a 3–D data volume on a 2–D monitor, we have developed a workstation (called UWGSP) capable of interactive multiplanar image display. The UWGSP was developed at the Image Processing Systems Laboratory at the University of Washington. Implemented in two IBM PC/AT prototyping cards with about 200 chips, it heavily utilizes the processing power of the Texas Instruments TMS34010 Graphics System Processor (GSP) and TMS32020 Digital Signal Processor (DSP)[7]. These two VLSI microprocessors, in concert with the host, provide an optimized and flexible imaging workstation (Figure **4**).

Selected UWGSP features include:

1) 512 × 512, 60Hz, noninterlaced color display.
2) Hardware zoom, roam, and cursor support.
3) Eight or twelve bits per pixel.
4) One video frame, three high-speed cache image frames, twelve host-resident frames (expandable to 48) and a separate graphics and cursor frame.
5) Fully programmable display windows: Up to fourteen frames may be windowed at a time in an arbitrary geometric pattern. Of these, up to three may be selected for simultaneous independent real-time pan and scroll. Window sizes and positions may be changed interactively.
6) Cine display up to thirty frames per second.
7) Programmable, variable-kernel two-dimensional convolution on a 512 × 512 image. Representative execution times: 3 × 3 kernel - three seconds; 11 × 11 kernel - nine seconds.
8) Interactive-rate geometric image transformations on a 512×512 image (rotation, warping or rubber-sheeting) in about ten seconds.
9) Two-dimensional Fast Fourier Transform (FFT) in fifteen seconds and Inverse Fast Fourier Transform (IFFT) in nineteen seconds.

The multiplanar image display software as it is currently implemented uses only MR images in two or three orthogonal planes, i.e., axial, coronal and sagittal. A 256 × 256 window is opened on the screen for each image axis in the study and a planar slice from the axis is placed in the window. The cursor is made active in a default window in the position that identifies the intersection of the other displayed orthogonal slices. As the cursor is moved in one plane, the image slices displayed in the other windows are updated in real time to correspond to the current location of the cursor. The cursor can be placed in any active window and will always be at the intersection of image slices displayed in the other windows. This allows the user to move about inside the image volume. Figure **5** shows a typical multiplanar MRI display. The coronal images shown in the top left window are reconstructed from the axial and sagittal image slices by means of interpolation.

The images from the MRI scanner are ported to the UWGSP system via a nine-track magnetic tape. The twelve-bit pixels are converted into eight-bit pixels. Windowing and leveling can be performed manually, or the first image in the study can be used to set the default window and level values. All other images in the study are processed with these default values unless the operator intervenes. After the window and level operations have been completed, information about image series within the study is displayed on the screen. The data headers associated with each image and each series are examined to extract the physical information required to align the images in the display windows. The multiplanar image display software also permits a chosen window to be enlarged by bilinear interpolation to full screen size, e.g. 512 × 512, taking about eight seconds. The mouse can be used to move the cursor to the desired location to find out its absolute x, y, z position. The developed system is general enough to be used in other applications to view 3–D data sets, for example in stereotactic neurosurgery.

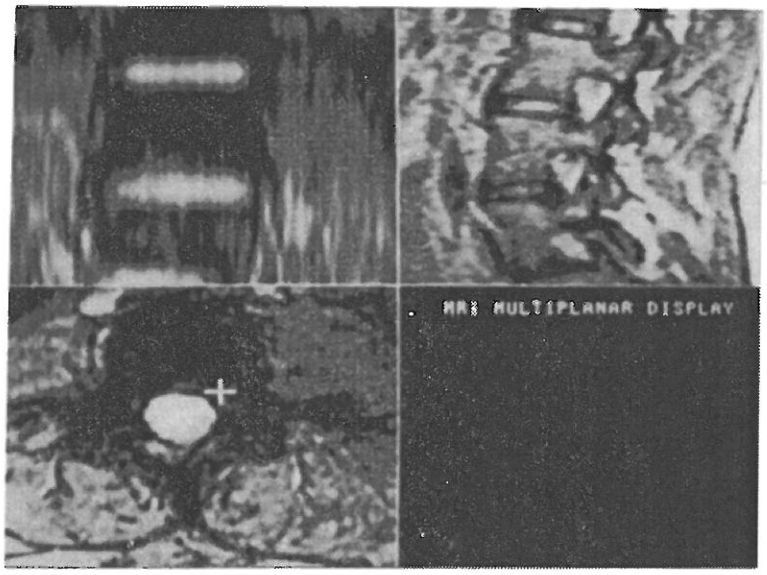

Figure 5 *Multiplanar display. Reformatted coronal (upper left), sagittal (upper right), and transaxial views.*

5. Conclusions

A large number of pathologic processes of the lower spine are not identified by current imaging and display systems. New technology is needed to improve diagnostic ability and then correlate these diagnoses with results of treatment, thus determining efficacy. Emphasis needs to be placed on soft tissues such as the intervertebral discs, ligaments and muscles of the spine, and MRI is likely to elucidate these tissues. Using 3–D displays of high-resolution MRI, physicians may now be able to identify injured or inflamed tissues and institute a directed treatment plan. Follow-up images could then be obtained to assess success.

Image processing tools which find edges and determine areas and volumes, along with interactive computer graphics, will improve the education of health professionals and open new areas of research in assessment of disease. Physicians who have utilized our image display systems note that the verifocal mirror system produces an instructive true 3–D picture which is useful for anatomical orientation and identification of feature anomalies. Further, the verifocal mirror system readily generates area and volume measurements which are analytically useful. The UWGSP system retains greyscale information which is of fundamental importance to physicians, and the cross–sectional data representation provides familiar views that are more typically helpful in diagnosis. Perhaps an optimal 3–D display system should incorporate the advantages of both systems, the verifocal and the UWGSP.

6. Acknowledgments

The authors wish to thank Jean Tkach who provided the original MRI data set obtained through the laboratory of Dr. Michael Modic at Case Western Reserve University. This work was generously supported by Siemens Medical Systems, Inc., Iselin, New Jersey.

7. References

1. M.T. Modic, R.W. Hardy, M.A. Weinstein, P.M. Duchesneau, D.M. Paushter and F. Boumphrey, "Nuclear magnetic resonance of the spine: clinical potential and limitation," *Neurosurgery 15*, 583-592 (1984).
2. J.L. Kelsey, A.A. White, H. Pastides and G.E. Bisbee, "The impact of musculoskeletal disorders on the population of the United States," *J. Bone Joint Surg. 61*, 959-964 (1979).
3. D.N. Kennedy and A.C. Nelson, "Three-dimensional display from cross-sectional tomographic images: an application to magnetic resonance imaging," *IEEE Trans. Med. Imag. MI-6*, 134-140 (1987).

4. R.M. Haralick, S.R. Sternberg and X. Zhuang, "Image analysis using mathematical morphology," *IEEE Trans. Pattern Anal. Machine Intel. PAMI-9*, 532-550 (1987).
5. R.M. Haralick, L.T. Watson, T.J. Laffey,"The Topographic Primal Sketch," *The International Journal of Robotic Research 2*, 50-71 (1983).
6. R.M. Haralick, "Digital Step Edges from Zero Crossings of Second Directional Derivatives," *IEEE Trans. Pattern Anal. Machine Intel. PAMI-6*, 58-68 (1984).
7. J.W. Chauvin, A.R. Steiner and Y. Kim, "Graphics and DSP IC's speed PC imaging," *ESD: The Elect. Syst. Design Mag. 17*, 49-51 (1987).